Single crystalline elastic constants of C15-type MAl_2 intermetallic compounds

by

Raymond John Schiltz, Jr.

A Dissertation Submitted to the
Graduate Faculty in Partial Fulfillment of
The Requirements for the Degree of
DOCTOR OF PHILOSOPHY

Major: Metallurgy

Approved:

Signature was redacted for privacy.

In Charge of Major Work

Signature was redacted for privacy.

For the Major Department

Signature was redacted for privacy.

For the Graduate College

Iowa State University
Ames, Iowa

1972

TABLE OF CONTENTS

INTRODUCTION

Background

The single crystalline elastic constants of a material are intimately connected with many of the physical, thermal, and mechanical properties of the material. Energetically, atoms in a periodic lattice can be described as sitting in a potential well with respect to spatial distribution, and the elastic constants are a measure of the curvature at the bottom of that potential well. Physically, the elastic constants are resultants of the interatomic force interactions in the lattice and are, therefore, closely related to lattice dynamics. The elastic constants are used to calculate the limiting slopes of phonon dispersion curves. Thermal properties are also dependent upon lattice dynamics. Debye temperatures obtained from elastic constants can be used in the calculation of thermodynamic quantities for temperatures at which the Debye model is valid. Elastic constants are, of course, fundamental in the study of the mechanical properties of materials undergoing elastic deformation. However, dislocation theory has made extensive use of the elastic properties in order to explain the phenomena associated with plastic deformation.

As may be seen in the compilations of Hearmon (1, 2), the amount of elastic constant data for single crystalline samples of pure metals and alloys with simple crystal structures is fairly extensive. However, the amount of elastic constant data for intermetallic compounds characterized by well defined stoichiometries and complex crystal structures is quite small. Single crystalline elastic constants have been determined for only 6 of the more than 380 Laves phases listed by Pearson (3). This

paucity of experimental data is largely due to the difficulty in the growing of a large single crystal of a compound that has a limited range of solubility. In many of these phases crystal growth is further complicated by severe homogeneity problems caused by incongruent melting of the phase. Solid state transformations in the crystal can make the growth of single crystal samples nearly impossible.

It is the intent of this research to measure the elastic constants of single crystals of several cubic Laves phase compounds with composition MAl_2. These compounds are extremely brittle and are susceptible to thermal shock. These factors tend to make crystal growth more difficult. On the other hand, these phases are very stable as evidenced by the high melting points, melt congruently, and have no phase transformations in the solid state. Trends in the elastic data from this family of compounds are expected to yield information about the nature and strength of bonding interactions in cubic Laves phases.

Laves Phases

The group of compounds known as Laves phases consists of three structure types: the cubic C15 ($MgCu_2$-type) and the hexagonal C14 ($MgZn_2$-type) and C36 ($MgNi_2$-type). The crystal structures of $MgCu_2$ and $MgZn_2$ were determined in 1927 by Friauf (4, 5) and that of $MgNi_2$ was determined in 1935 by Laves and Witte (6). As of 1967 Pearson (3) lists over 380 Laves phases of which 196 are cubic. Laves was the first to emphasize the structural relationships among the three structure types. This, in combination with the large amount of effort that he has devoted to the study of these structures (7), has led to the application of the name "Laves phases" for

these structures.

There is a significant body of evidence that the size factor is one of the dominant considerations contributing to the formation of these compounds. If the phase stoichiometry is given by AB_2 then A represents the large species and B represents the small species. The characteristic symmetry of a cubic Laves phase is that of space group Fd3m and there are 24 atoms per unit cell. Eight A atoms are located at 0 0 0, 1/4 1/4 1/4 plus the face-centering translations, and sixteen B atoms are found at 5/8 5/8 5/8, 5/8 7/8 7/8, 7/8 5/8 7/8, 7/8 7/8 5/8 plus the face-centering translations. An A atom has 12 nearest neighbor B atoms ($d_{AB} = a_o\sqrt{11}/8 = 0.415\ a_o$) and four next nearest neighbor A atoms ($d_{AA} = a_o\sqrt{3}/4 = 0.432\ a_o$). Each B atom has 6 nearest neighbor B atoms ($d_{BB} = a_o\sqrt{2}/4 = 0.353\ a_o$) and 6 next nearest neighbor A atoms.

Assuming A-A and B-B contacts in a hard sphere approximation the ideal radius ratio for this structure is

$$r_A/r_B \text{ (ideal)} = \sqrt{3}\ /\sqrt{2} = 1.225\ . \qquad (1)$$

If $r_A/r_B<1.225$, then only B-B contacts are present. Conversely, if $r_A/r_B>1.225$, then only A-A contacts are present. There are never A-B contacts in this hard sphere model.

It has been noted that the elastic constants are closely related to interatomic forces in solids and, thus, understanding of force interactions can be enhanced by the systematic examination of the elastic constants of these Laves phases. Elastic constant data for binary cubic Laves phases are available only for $ZrCo_2$ (8), $HfCo_2$ (8), UCo_2 (9), and $MgCu_2$ (10), while

for hexagonal Laves phases only $CaMg_2$ (11) and $MgZn_2$ (12) have been investigated. Shannette and Smith (13) have reported the elastic constants of the psuedo-binary $MgCu_2$-$MgZn_2$ system.

Several factors are usually considered in the selection of a series of compounds for elastic constant study. The most important is whether or not single crystals of the phases can be grown. Other considerations are reactivity, ease of handling and availability of starting materials. There are 21 known cubic Laves phases of stoichiometry MAl_2 and these phases are all congruently melting, readily prepared, and nearly inert to atmospheric contamination at room temperature. The M elements that form these phases are Ca, Sc, Y, La through Lu, U, Pu, and Np. Aluminum of high purity is readily available. In this laboratory, calcium and the rare earths are available, and the purity of these metals is believed to be the best in the world.

These phases have been the object of considerable study, and literature is available detailing their specific heats (e.g., 14, 15, 16), electrical resistivities (e.g., 17, 18, 19), and magnetic behaviors (e.g., 20, 21, 22). NMR studies of these phases have been concerned with properties of pure phases and of dopant impurities (e.g., 23, 24, 25). Neutron diffraction techniques have been employed (e.g., 26, 27, 28) to investigate the magnetic structures of some of these phases.

The Debye temperatures are of particular interest in this investigation. The behavior of the Debye temperatures of Laves phases has been found to correlate with the radius ratios (29). Testing of this correlation for the RAl_2 phases with specific heat data is complicated by the

presence of the magnetic transformations which have been observed in most of these phases. The Debye parameter of a solid is associated strictly with the lattice contribution to the heat capacity. Therefore, evaluation of Debye temperatures from specific heat data is normally done with lesser reliability if magnetic or other extraneous contributions are present. This is not true of Debye temperatures from elasticity data, and Alers (30) has shown that Debye temperatures from elastic constant measurements are generally more reliable than those calculated from specific heat data.

Crystal Elasticity

The formal concepts of elasticity are well defined and have been surveyed by Love (31), Nye (32) and Huntington (33). These concepts are based on pure stress-pure strain considerations with a coordinate system chosen so as to abstract rotational and translational changes. Under these conditions the linear relationship between stress and strain is known as Hooke's Law and is

$$\sigma_i = C_{ij}\epsilon_j \ , \tag{2}$$

where the indices range from 1 to 6 and repeated indices indicate summation. The σ_i are the six independent stress components and the ϵ_j are the six independent strain components as defined by:

$$\epsilon_1 = \frac{\partial u}{\partial x} \ , \ \epsilon_2 = \frac{\partial v}{\partial y} \ , \ \epsilon_3 = \frac{\partial w}{\partial z}$$

$$\epsilon_4 = \frac{\partial v}{\partial z} + \frac{\partial w}{\partial y} \ , \ \epsilon_5 = \frac{\partial u}{\partial z} + \frac{\partial w}{\partial x} \ , \ \epsilon_6 = \frac{\partial u}{\partial y} + \frac{\partial v}{\partial x} \ , \tag{3}$$

where u, v, and w are displacements in the x, y, and z directions, respectively. The C_{ij} are elements of the elastic constant matrix and, as shown in the foregoing references (31, 32, 33), there are at most 21 independent elastic constants. This number is reduced by symmetry constraints, and the symmetry constraints of the cubic crystal class reduce the number of independent elastic constants to three. The elastic constant matrix for a cubic crystal is

$$\left[C_{ij}\right] = \begin{bmatrix} C_{11} & C_{12} & C_{12} & 0 & 0 & 0 \\ C_{12} & C_{11} & C_{12} & 0 & 0 & 0 \\ C_{12} & C_{12} & C_{11} & 0 & 0 & 0 \\ 0 & 0 & 0 & C_{44} & 0 & 0 \\ 0 & 0 & 0 & 0 & C_{44} & 0 \\ 0 & 0 & 0 & 0 & 0 & C_{44} \end{bmatrix}. \tag{4}$$

The dynamics of the stress-strain relationship may be described by expressing Newton's Second Law of Motion in the following manner:

$$\rho\frac{\partial^2 u}{\partial t^2} = \frac{\partial\sigma_1}{\partial x} + \frac{\partial\sigma_6}{\partial y} + \frac{\partial\sigma_5}{\partial z} \tag{5a}$$

$$\rho\frac{\partial^2 v}{\partial t^2} = \frac{\partial\sigma_6}{\partial x} + \frac{\partial\sigma_2}{\partial y} + \frac{\partial\sigma_4}{\partial z} \tag{5b}$$

$$\rho\frac{\partial^2 w}{\partial t^2} = \frac{\partial\sigma_5}{\partial x} + \frac{\partial\sigma_4}{\partial y} + \frac{\partial\sigma_3}{\partial z} \quad , \tag{5c}$$

where ρ is density and t is time. Substitution of Equations 2, 3, and 4 in Equations 5 results in the equations of motion for a cubic crystal:

$$\rho\frac{\partial^2 u}{\partial t^2} = C_{11}\frac{\partial^2 u}{\partial x^2} = C_{12}\left(\frac{\partial^2 v}{\partial x\partial y} + \frac{\partial^2 w}{\partial x\partial z}\right) + C_{44}\left(\frac{\partial^2 u}{\partial z^2} + \frac{\partial^2 u}{\partial y^2} + \frac{\partial^2 v}{\partial x\partial y} + \frac{\partial^2 w}{\partial x\partial z}\right) \tag{6a}$$

$$\rho\frac{\partial^2 v}{\partial t^2} = C_{11}\frac{\partial^2 v}{\partial y^2} + C_{12}\left(\frac{\partial^2 u}{\partial x\partial y} + \frac{\partial^2 w}{\partial y\partial z}\right) + C_{44}\left(\frac{\partial^2 u}{\partial x\partial y} + \frac{\partial^2 v}{\partial x^2} + \frac{\partial^2 v}{\partial z^2} + \frac{\partial^2 w}{\partial y\partial z}\right) \tag{6b}$$

$$\rho\frac{\partial^2 w}{\partial t^2} = C_{11}\frac{\partial^2 w}{\partial z^2} + C_{12}\left(\frac{\partial^2 u}{\partial x\partial z} + \frac{\partial^2 v}{\partial y\partial z}\right) + C_{44}\left(\frac{\partial^2 u}{\partial x\partial z} + \frac{\partial^2 v}{\partial y\partial z} + \frac{\partial^2 w}{\partial x^2} + \frac{\partial^2 w}{\partial y^2}\right) . \tag{6c}$$

Solutions of these equations depend upon the boundary conditions, and the plane wave solution is given by Kittel (34):

$$u = u_o \exp[i(K_1 x + K_2 y + K_3 z - \omega t)] \tag{7a}$$

$$v = v_o \exp[i(K_1 x + K_2 y + K_3 z - \omega t)] \tag{7b}$$

$$w = w_o \exp[i(K_1 x + K_2 y + K_3 z - \omega t)] \tag{7c}$$

where u_o, v_o, and w_o are amplitudes of the corresponding waves, ω is the angular frequency, and K is the wave number vector such that $K_1^2 + K_2^2 + K_3^2 = K^2$.

Plane waves travelling in high symmetry directions exhibit normal modes and in the particular case of the [110] direction there is no degeneracy. In that case $K_1^2 = K_2^2 = \frac{1}{2}K^2$ and $K_3 = 0$. Kittel (34) has shown that substitution of these K_i and Equations 7 into Equations 6 results in the following equations:

$$\rho V_L^2 = \tfrac{1}{2}(C_{11} + C_{12} + 2C_{44}) \tag{8a}$$

$$\rho V_s^2 = \tfrac{1}{2}(C_{11} - C_{12}) \tag{8b}$$

$$\rho V_t^2 = C_{44} \tag{8c}$$

where ρ is the density, V_L is the velocity of a longitudinal wave, and V_s and V_t are the velocities of transverse waves polarized in the $[1\bar{1}0]$ and [001] directions, respectively. Equations 8 allow the calculation of the elastic constants of a cubic crystal from measurements made from the velocities of wave propagation along a [110] direction.

EXPERIMENTAL PROCEDURE

Specimen Preparation

Single crystals of $CaAl_2$, YAl_2, $LaAl_2$, and $GdAl_2$ were grown to produce samples for elastic constant determinations. Alloys were prepared from aluminum that was certified to be 99.999% pure from Cominco American, Inc., and from high purity Ca, Y, La, and Gd that had been prepared at the Ames Laboratory. The major impurities in the aluminum were 5 ppm Fe and 2 ppm Cu by weight. Analyses of the other metals are presented in Table 1. Before preparing the alloys the aluminum was cleaned in a hot saturated NaOH aqueous solution. The calcium had been stored in a purified argon atmosphere so that no surface cleaning was required. The remaining metals were cleaned by electropolishing in a methanol-6% perchloric acid electrolyte at $-70^{\circ}C$.

The MAl_2 phases are all congruently melting and, since accurate melting points were needed for crystal growth, McMasters (35) was kind enough to determine the melting points of several MAl_2 phases by differential thermal analysis. These melting points with a precision of $\pm$ $10^{\circ}C$ are as follows:

$ScAl_2$ -- $1355^{\circ}C$	$GdAl_2$ -- $1495^{\circ}C$
YAl_2 -- $1480^{\circ}C$	$ErAl_2$ -- $1502^{\circ}C$
$LaAl_2$ -- $1370^{\circ}C$	$LuAl_2$ -- $1465^{\circ}C$
$PrAl_2$ -- $1455^{\circ}C$	

These compounds all exhibit very limited solid solubility and so it is important that the alloys be prepared with the proper stoichiometry.

Table 1. Chemical analyses of the constituent metals

Element	Concentration in wt. ppm			
	Ca*	Y**	La**	Gd**
H	100		3.4	1.4
B		<.05		.03
C	30	50	37	12
N	3	10	15	4
O	30	40	30	107
F		.4	13	4
Na		.8	.1	1
Mg	300	.5	<.5	.7
Al	20	300	≤3	≤20
Si		≤1	2	≤.7
P		<.07		≤.1
S		<4		<10
Cl		1	10	4
K		1	.5	.7
Ca	10^6	.4	.1	2
Sc		<10	.1	3
Ti		.2	<2	1
V		.06	.1	≤.4
Cr	2	.2		2
Mn	10	.2		.2
Fe	2	30	3.1	8.4
Co		.07	<.1	.06
Ni	2	20	9	3
Cu	2	50	1	.5
Zn		.5	.1	<.05
Ga		<.08		<.1
Ge		<.08		
As		<.09		
Se		<.09		
Br		<.09		
Kr		<.1		
Rb		<.1		
Sr	500	$<1_6$		
Y		10	7	2
Zr		<2		<.4
Mo		<1		
Ru		<.6		
Rh		<.2		<.2

*Analysis for Ca is for a typical production run at Ames Laboratory.

**Analyses for Y, La, and Gd were made by mass spectrometery for all elements except for H,C, N, O, F, Fe, Ni, and Cr. Analyses for H, N, and O were by vacuum fusion analysis and those for carbon were by combustion analysis. Fluorine was determined as distilled fluosilicic acid. Fe, Ni, and Cr were determined by absorption techniques.

Table 1. (Continued)

Element	Concentration in wt. ppm			
	Ca*	Y**	La**	Gd**
Pd				<.4
Ag		<2		<.2
Cd		<.4		<.2
In		<1		<.08
Sn				<.4
Sb		<2		<.08
Te		<.8		<.2
I		<.8		<.2
Cs		<.4		<.06
Ba	400	<.8		<.08
La		7.4	10^6	1
Ce		8.7	9	.7
Pr		3.4	6	3.2
Nd		4.7	1.6	8
Sm		.8	<.7	<.3
Eu		<.1	<.1	<.08
Gd		14	2.7	10^6
Tb		4.1	10	≤3
Dy		25	≤.3	1.8
Ho		15	.8	<.5
Er		10	<.2	2.6
Tm		<.2	<.1	≤3
Yb		<.4	<.2	≤10
Lu		12	≤1	≤2
Hf		<.4		<1
Ta		300	7	≤1
W		4	<2	≤1
Re		<.4		<.8
Os		<.4		<2
Ir		<.4		<.8
Pt		≤4	.8	<1
Au		<.4		<.2
Hg		<.7		<.2
Tl		<.2		<.1
Pb		5	<.2	.3
Bi		<.2		<.08
Th		<.8	<.2	<.3
U		<.8	<.3	<.2

To prepare YAl_2, $LaAl_2$, and $GdAl_2$ alloys, stoichiometric weights of Al and rare earth were alloyed by arc melting in a purified argon atmosphere according to the procedure described by Hungsberg and Gschneidner (16). $CaAl_2$ was prepared in a somewhat different manner because the high vapor pressure of calcium precludes arc melting. Stoichiometric amounts of Ca and Al were weighed under a purified argon atmosphere and sealed in a 1.00 inch diameter tantalum crucible under one atmosphere of argon. The melting point of $CaAl_2$ is listed by Pearson (36) as 1079°C, so the alloy was heated to 1200° in an induction furnace. It was held at that temperature for 15 minutes to ensure melting and to facilitate homogenization of the liquid alloy and was subsequently cooled to room temperature. Since $CaAl_2$ is very brittle, hitting the crucible several sharp blows with a hammer was sufficient to fragment the alloy and allow it to be removed from the crucible. Alloy weights ranged from 23 g for $CaAl_2$ to 73 g for $GdAl_2$ and constituent elements were weighed to $\pm$ 1 mg.

Since single crystals were to be grown in a vacuum furnace by the Bridgman technique, pointed crucibles were necessary. Pointed tantalum crucibles were manufactured by spinning a 60° cone on one end of 5 inch long, 0.75 inch diameter tantalum tubes. The tips of these cones were sealed by TIG welding. Each alloy was crushed before loading. In order to prevent loss of aluminum at high temperatures the crucibles were sealed at a pressure of 10^{-5} torr by electron beam welding. The Bridgman furnace was heated by passing current through a molybdenum resistance element which was wrapped around an alumina core. Pressures in the furnace chamber were typically 10^{-5} to 10^{-7} torr during operation. During a run,

the sample temperature was monitored by a platinum vs. platinum -10% rhodium thermocouple located near the tip of the crucible.

In order to grow single crystals, each sample was heated to approximately 100°C above its melting point. After approximately one hour in the molten state, the sample was lowered into the cool zone of the furnace at a rate of 1.5 cm per hour. In this manner crystals were obtained which were of sufficient size to produce finished samples approximately 1.0 cm in diameter and 0.56 to 1.06 cm thick in the [110] direction.

Crystal orientation was accomplished by means of the back reflection Laue technique of Meyerhoff, Bailey, and Smith (37). The crystal was solidly affixed to the goniometer head with an electrically conductive mixture of Duco cement and graphite powder. When a [110] direction was accurately located, the goniometer head was transferred to a Sparkatron electromachining apparatus in which parallel faces were cut perpendicular to a [110] direction. The (110) faces were hand lapped through 600 grit polishing paper with the aid of a grinding jig. Removal of residual worked metal was accomplished by electropolishing approximately 0.005 cm from the thickness. This procedure produced crystal faces that were flat and parallel to within 0.0003 cm and with face normals within 0.5° of the [110] direction.

Density Determination

The density of any MAl_2 sample can be calculated if the lattice parameter of the compound is known. Density is related to the lattice parameter in the following way:

$$\rho = \frac{8(W_M + 2W_{Al})}{.60225\ a_o^3} \quad , \tag{9}$$

where ρ is the density in g/cm^3, W_M and W_{Al} are the atomic weights of the metals M and Al, respectively, and a_o is the lattice parameter in angstroms. In this investigation atomic weights were taken from the Handbook of Chemistry and Physics (38).

In order to calculate densities, precision lattice parameters of the elastic constant specimens were measured at room temperature. Measurements were made with a General Electric diffractometer and copper radiation. Values for the Kα and Kβ wavelengths were taken from the tabulation of Cullity (39). A 1^o beam slit, a medium resolution detector Soller slit, and a 0.1^o detector slit were used in the diffractometer. The crystal was located in the goniometer with the (110) face in diffracting position. This orientation was attained by use of the rotational and translational adjustments of the goniometer head in combination with adjustment of an independent omega motion furnished by a special base for the goniometer head.

Proper alignment was indicated by the presence of smooth, symmetrical Bragg reflections (with $\alpha_1 - \alpha_2$ separation usually at 2θ values as low as 32^o) and by the near-zero slopes of the linear least squares fit of the data in the Nelson-Riley extrapolation (40). The diffracted intensities were measured with a scintillation counter during scans at 0.2^o 2θ per minute and were recorded on a strip chart recorder driven by a rate meter with 0.5 second time constant. Locations of peaks were measured at one-half peak height and data were accumulated for all available hh0

reflections. Where possible, the $K\alpha_1$ and $K\alpha_2$ peaks were resolved and used in the calculation of lattice parameters. Precision lattice parameters were calculated by a Nelson-Riley extrapolation (40) with a linear least squares fit to the data. The Nelson-Riley function has been shown by Otte (41) to be a good extrapolation function for this diffraction geometry. The validity of this procedure is evidenced by small standard deviations and reproducibility. Three independent determinations of the lattice parameter of $LaAl_2$ were made and all results agreed within experimental precision. The lattice parameters determined in this manner for $CaAl_2$, YAl_2, $LaAl_2$, and $GdAl_2$ are in reasonable agreement with those reported by other investigators (e.g., 3, 16, 42, 43, 44).

Ultrasonic Wave Velocity Determination

In order to calculate elastic constants from Equations 8 it was necessary to determine the velocities of the elastic plane waves. The velocities of waves propagating in the [110] direction were calculated from the following relation,

$$V = \frac{2h}{t} \quad , \tag{10}$$

where h is the thickness of the crystal in the [110] direction, t is the transit time required for the wave to travel twice the thickness of the crystal and V is the wave velocity.

The thickness of the sample in the [110] direction was measured at room temperature with a micrometer with direct readings to 0.0001 inch. Five measurements were made of each thickness and were averaged to obtain a representative value.

Transit times of the elastic waves were measured by the pulse-echo-overlap method with the apparatus described by Eshelman (45). X-cut and Y-cut quartz transducers with resonant frequencies of 10 MHz were used to generate longitudinal and transverse waves in the samples. Transit times of from 2.0 to 7.1 microseconds were measured with a precision of $\pm$ 0.001 microsecond over the temperature range 4.2 to 300 K. Sample temperatures were determined by the use of thermocouples whose junctions were held in intimate contact with the specimen with tape. These thermocouples were constructed from small diameter wires ($\leq$ 6 mil) in order to minimize thermal inertia in the thermocouple. Copper *vs.* constantan was used over the range 40-300 K and Au-0.03 Fe *vs.* Ag was used over the range 4.2 to 50 K. Nonaq stopcock grease served as a bonding agent between the quartz transducers and the samples over the entire temperature range for longitudinal modes and over the range 4.2 to 270 K for transverse modes. Salol (phenyl salicylate) was used as the bonding agent for transverse modes at higher temperatures.

In order to measure transit times over the temperature range 4.2 to 100 K, each sample was suspended in a sample holder in a cryostat. Sufficient liquid helium was transferred into the cryostat to immerse the specimen and specimen holder. The transit time at 4.2 K was measured while the crystal was immersed in liquid helium at atmospheric pressure. Transit times were measured in the range 5 to 80 K as the helium boiled off and the temperature of the sample increased over a period of several hours. The temperature change was not rapid, so any temperature gradients in the sample were small. Errors due to any small gradients would be

insignificant because the transit time itself is a slowly changing function of temperature. Since an individual transit time measurement requires but a few seconds, the sample was at essentially constant temperature during each measurement.

Transit times over the temperature range 77 to 300 K were measured with the sample holder inserted in a closely fitting copper heat reservoir. A resistance heater was wrapped around the heat reservoir for temperature control. This assembly was suspended in a dewar above liquid nitrogen and cooled by the nitrogen gas evolved by boiling. A second heater was submerged in the liquid nitrogen to control the boiling rate. Measurements could be made during either heating or cooling of the sample. Measurements were taken at 77 K with the sample immersed in liquid nitrogen.

The pulse-echo-overlap technique was developed by May (46) and Papadakis (47) and is a modification of the basic pulse-echo method of Huntington (48). The pulse-echo method requires a measurement of the time between successive echoes in an echo train following an initial pulse. In the pulse-echo-overlap method this time measurement is accomplished by varying the triggering rate of an oscilloscope until overlap of successive echoes is seen on the oscilloscope screen. Another popular modification of the basic pulse-echo method is the pulse-superposition method of McSkimmin (49) in which the repetition rate of a pulsed oscillator is varied until a resonance condition is reached as determined by an oscilloscope display. As compared with the basic pulse-echo method, both of these modifications have the advantages of increased accuracy and

speed. This latter advantage obviates the need to control temperature accurately over relatively long periods of time and allows the accumulation of data at much smaller temperature intervals in less time than is possible for the pulse-echo technique. In addition, the overlap method has two important advantages over the superposition method. First, the overlap method requires cycle-by-cycle investigation of the echoing wave packets. This allows a definitive choice of the leading edges of the echoes. Such a definitive choice is not possible in the superposition method. Second, the superposition method is limited in the minimum transit times that can be measured by the high frequency that is required to drive the pulsed oscillator. The overlap method is limited only by the length of the pulse envelope, and this usually allows the investigation of smaller samples.

RESULTS

Transit time measurements were made over the temperature range 4.2 to 300 K for the cubic Laves phase compounds $CaAl_2$, YAl_2, $LaAl_2$, and $GdAl_2$. Only one crystal of each phase was involved. The elastic constants C_L, C_{44}, and C' were evaluated from the transit times from the relationships in Equations 8 by the use of the lattice parameters, calculated densities, and crystal dimensions which are listed in Table 2. Plots of these elastic constants as functions of temperature are presented in Figures 1 through 4. It is readily seen from these plots that the data points are closely spaced and the experimental scatter is small. This allows smooth curves to be drawn to fit the data without resorting to analytical curve fitting techniques. These curves were drawn with zero slope at 0 K as required by the Third Law of Thermodynamics. The apparent steps in the plots of C_L near 0 K in Figure 1 represent the limit of resolution in the transit time measurements for that wave mode and are not representative of actual discontinuties in the elastic behavior.

Smoothed values were read from these curves and were used to calculate C_{11}, C_{12}, and the elastic anisotropy ratio, $A = C_{44}/C'$. The measured and calculated elastic constants for $CaAl_2$, YAl_2, $LaAl_2$, and $GdAl_2$, are presented in Tables 3, 4, 5, and 6, respectively. The unusual behavior shown for $GdAl_2$ near 165 K is a result of the ferromagnetic ordering transformation that has been reported near this temperature (18, 50, 51, 52). The dashed lines in Figure 4 are extrapolations of the elastic constants of magnetically disordered $GdAl_2$ to 0 K. Elastic constants calculated from these extrapolated values are included in Table 6.

Table 2. Lattice parameters, densities and specimen thicknesses for the elastic constant specimens at room temperature

Compound	a_o (Å)	ρ (g/cm^3)	h (inch)
$CaAl_2$	8.0404 ± 0.0001	2.4032 ± 0.0001	0.2811 ± 0.0001
YAl_2	7.8687 ± 0.0001	3.8953 ± 0.0002	0.3428 ± 0.0001
$LaAl_2$	8.1495 ± 0.0001	4.7338 ± 0.0001	0.4061 ± 0.0001
$GdAl_2$	7.9053 ± 0.0001	5.6793 ± 0.0002	0.2213 ± 0.0001

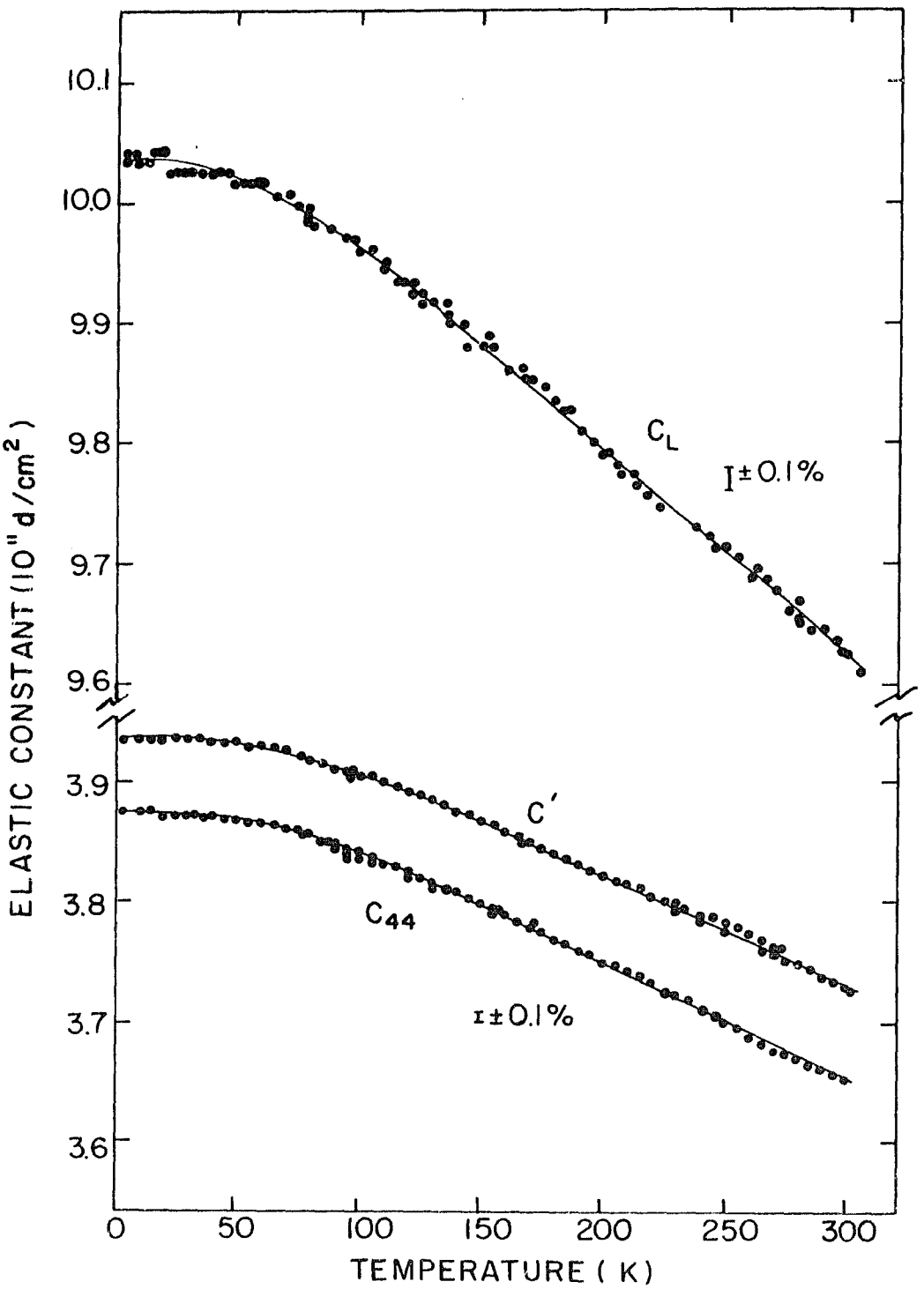

Figure 1. Single crystalline elastic constant data for $CaAl_2$

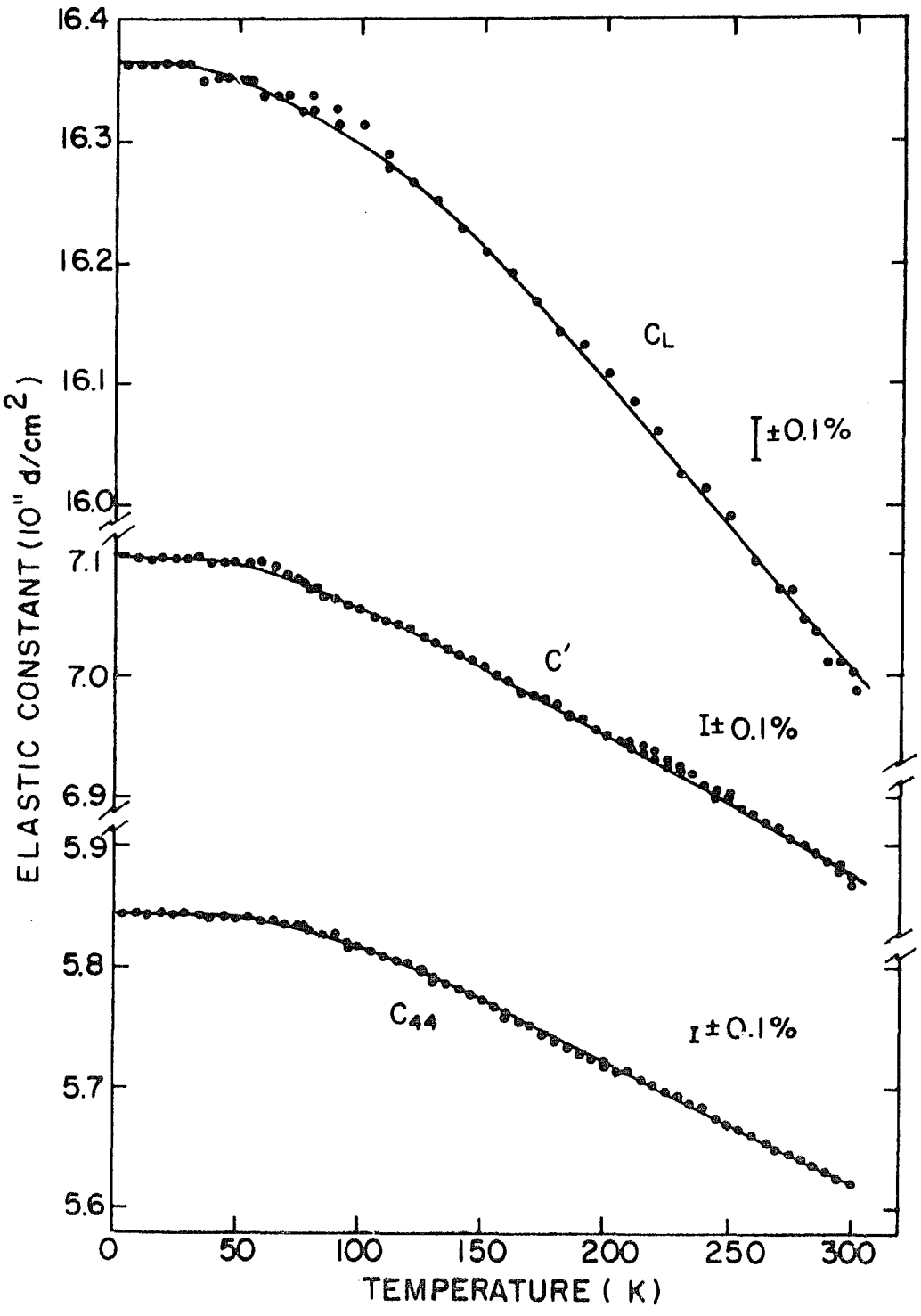

Figure 2. Single crystalline elastic constant data for YAl_2

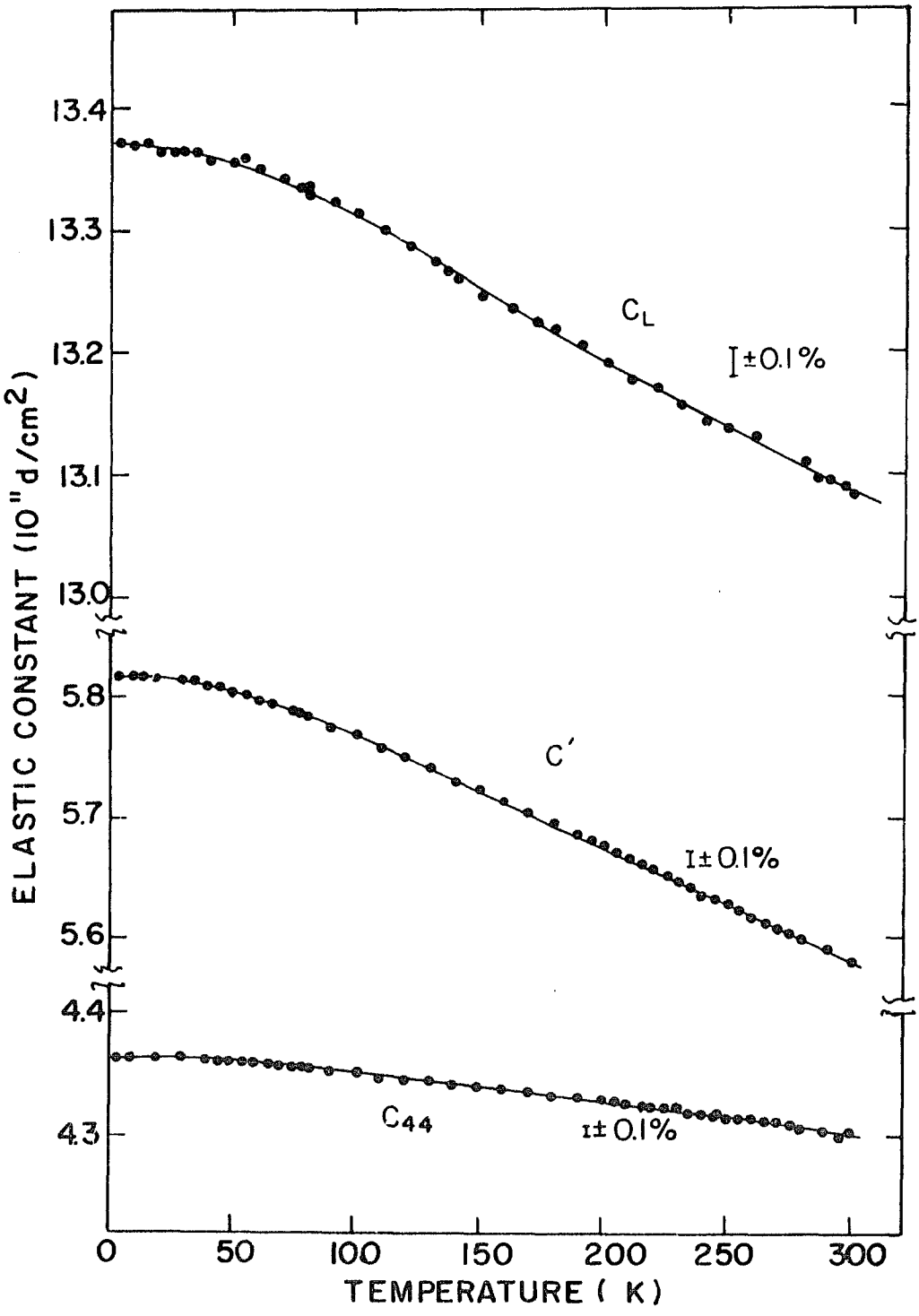

Figure 3. Single crystalline elastic constant data for $LaAl_2$

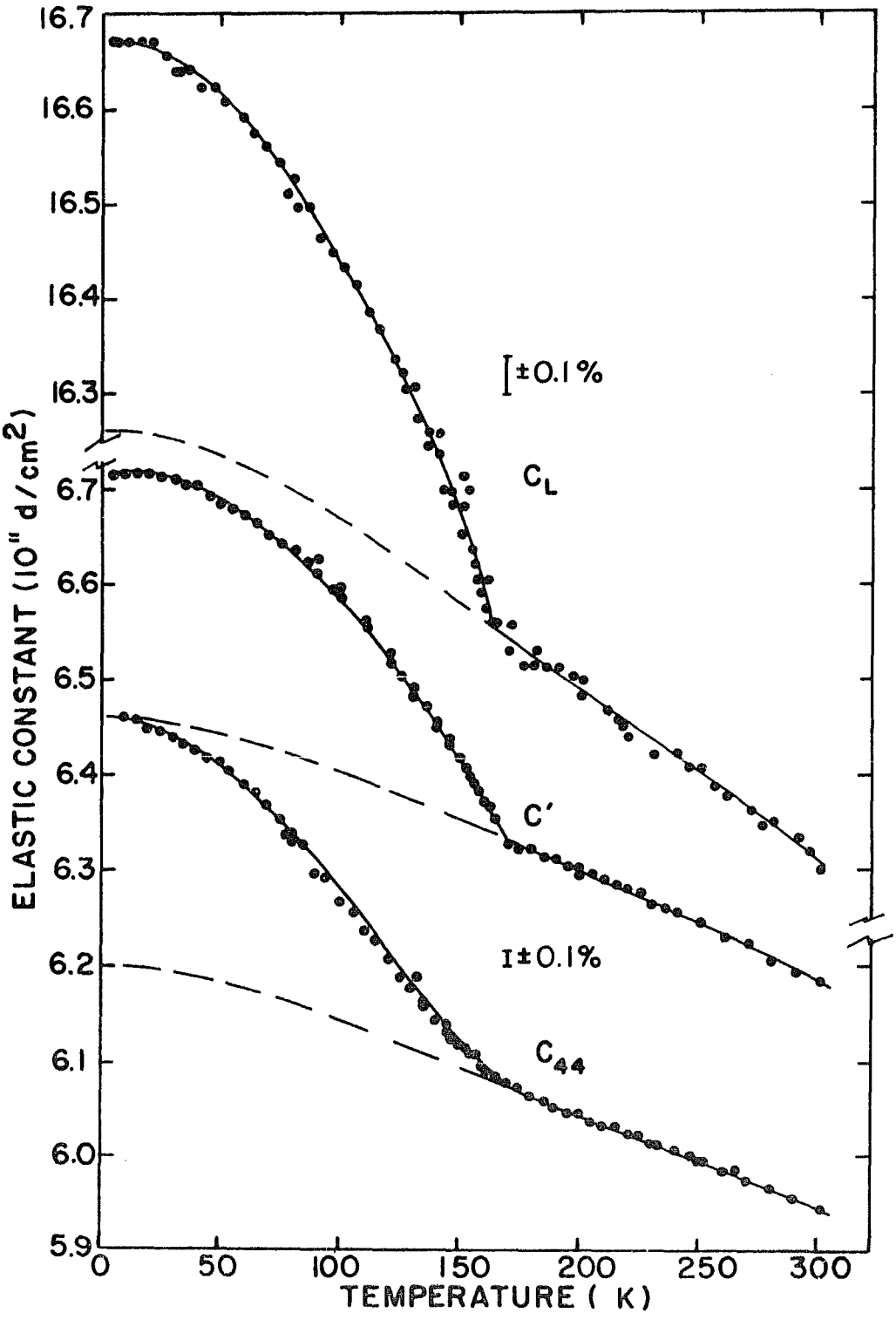

Figure 4. Single crystalline elastic constant data for $GdAl_2$. Dashed lines represent extrapolation of magnetically disordered phase

Table 3. Smoothed values for the elastic constants of single crystalline $CaAl_2$ in d/cm^2 ($A = C_{44}/C'$ is dimensionless)

T(K)	C_{11} ±0.014	C_{12} ±0.014	C_{44} ±0.002	C' ±0.002	C_L ±0.009	A ±0.001
4	10.101	2.231	3.875	3.935	10.041	.985
10	10.100	2.230	3.875	3.935	10.040	.985
20	10.098	2.230	3.874	3.934	10.038	.985
30	10.094	2.226	3.873	3.934	10.033	.984
40	10.089	2.225	3.871	3.932	10.028	.984
50	10.082	2.222	3.869	3.930	10.021	.984
60	10.076	2.220	3.865	3.928	10.013	.984
70	10.065	2.217	3.861	3.924	10.002	.984
80	10.055	2.217	3.855	3.919	9.991	.984
90	10.043	2.217	3.848	3.913	9.978	.983
100	10.031	2.217	3.840	3.907	9.964	.983
110	10.017	2.217	3.832	3.900	9.949	.983
120	10.000	2.216	3.824	3.892	9.932	.983
130	9.985	2.217	3.814	3.884	9.915	.982
140	9.968	2.218	3.805	3.875	9.898	.982
150	9.951	2.219	3.796	3.866	9.881	.982
160	9.934	2.220	3.787	3.857	9.864	.982
170	9.918	2.222	3.777	3.848	9.847	.982
180	9.901	2.223	3.768	3.839	9.830	.982
190	9.885	2.225	3.758	3.830	9.813	.981
200	9.868	2.226	3.749	3.821	9.796	.981
210	9.852	2.228	3.739	3.812	9.779	.981
220	9.835	2.229	3.730	3.803	9.762	.981
230	9.818	2.230	3.721	3.794	9.745	.981
240	9.802	2.232	3.711	3.785	9.728	.980
250	9.785	2.233	3.702	3.776	9.711	.980
260	9.769	2.235	3.692	3.767	9.694	.980
270	9.752	2.236	3.683	3.758	9.677	.980
280	9.735	2.237	3.674	3.749	9.660	.980
290	9.719	2.239	3.664	3.740	9.643	.980
300	9.702	2.240	3.655	3.731	9.626	.980

Table 4. Smoothed values for the elastic constants of single crystalline YAl_2 in d/cm^2 ($A = C_{44}/C'$ is dimensionless)

T(K)	C_{11} ±0.018	C_{12} ±0.018	C_{44} ±0.003	C' ±0.004	C_L ±0.012	A ±0.001
4	17.619	3.421	5.845	7.099	16.365	.823
10	17.619	3.421	5.845	7.099	16.365	.823
20	17.617	3.421	5.844	7.098	16.363	.823
30	17.613	3.419	5.844	7.097	16.360	.823
40	17.607	3.417	5.843	7.095	16.355	.824
50	17.600	3.416	5.841	7.092	16.349	.824
60	17.590	3.414	5.839	7.088	16.341	.824
70	17.578	3.414	5.836	7.082	16.332	.824
80	17.565	3.415	5.831	7.075	16.321	.824
90	17.551	3.419	5.825	7.066	16.310	.824
100	17.537	3.421	5.818	7.058	16.297	.824
110	17.520	3.424	5.811	7.048	16.283	.824
120	17.504	3.426	5.802	7.039	16.267	.824
130	17.487	3.429	5.793	7.029	16.251	.824
140	17.467	3.431	5.783	7.018	16.232	.824
150	17.448	3.432	5.773	7.008	16.213	.824
160	17.426	3.432	5.763	6.997	16.192	.824
170	17.403	3.431	5.753	6.986	16.170	.824
180	17.382	3.430	5.742	6.976	16.148	.823
190	17.358	3.428	5.732	6.965	16.125	.823
200	17.334	3.426	5.722	6.954	16.102	.823
210	17.309	3.423	5.712	6.943	16.078	.823
220	17.284	3.420	5.702	6.932	16.054	.823
230	17.259	3.419	5.692	6.920	16.031	.823
240	17.234	3.416	5.682	6.909	16.007	.822
250	17.209	3.415	5.672	6.897	15.984	.822
260	17.184	3.412	5.662	6.886	15.960	.822
270	17.160	3.410	5.652	6.875	15.937	.822
280	17.134	3.408	5.642	6.863	15.913	.822
290	17.109	3.405	5.632	6.852	15.889	.822
300	17.084	3.404	5.622	6.840	15.866	.822

Table 5. Smoothed values for the elastic constants of single crystalline $LaAl_2$ in d/cm^2 ($A = C_{44}/C'$ is dimensionless)

T(K)	C_{11}	C_{12}	C_{44}	C'	C_L	A
	±0.010	±0.010	±0.001	±0.002	±0.007	±0.001
4	14.821	3.193	4.363	5.814	13.370	.750
10	14.821	3.193	4.363	5.814	13.370	.750
20	14.819	3.191	4.362	5.814	13.367	.750
30	14.815	3.191	4.361	5.812	13.364	.750
40	14.808	3.192	4.360	5.808	13.360	.751
50	14.798	3.192	4.359	5.803	13.354	.751
60	14.787	3.193	4.358	5.797	13.348	.752
70	14.774	3.194	4.357	5.790	13.341	.753
80	14.761	3.195	4.355	5.783	13.333	.753
90	14.745	3.197	4.353	5.774	13.324	.754
100	14.728	3.196	4.351	5.766	13.313	.755
110	14.709	3.195	4.349	5.757	13.301	.755
120	14.688	3.194	4.347	5.747	13.288	.756
130	14.669	3.191	4.345	5.739	13.275	.757
140	14.651	3.191	4.342	5.730	13.263	.758
150	14.630	3.190	4.340	5.720	13.250	.759
160	14.611	3.189	4.338	5.711	13.238	.760
170	14.592	3.188	4.336	5.702	13.226	.760
180	14.573	3.187	4.334	5.693	13.214	.761
190	14.554	3.186	4.332	5.684	13.202	.762
200	14.537	3.187	4.329	5.675	13.191	.763
210	14.519	3.187	4.327	5.666	13.180	.764
220	14.502	3.188	4.325	5.657	13.170	.765
230	14.486	3.190	4.322	5.648	13.160	.765
240	14.468	3.190	4.320	5.639	13.149	.766
250	14.452	3.192	4.317	5.630	13.139	.767
260	14.435	3.193	4.314	5.621	13.128	.767
270	14.417	3.195	4.312	5.611	13.118	.768
280	14.401	3.197	4.309	5.602	13.108	.769
290	14.384	3.198	4.306	5.593	13.097	.770
300	14.368	3.200	4.303	5.584	13.087	.771

Table 6. Smoothed values for the elastic constants of single crystalline $GdAl_2$ in d/cm^2 ($A = C_{44}/C'$ is dimensionless)

T(K)	C_{11} ±0.024	C_{12} ±0.024	C_{44} ±0.004	C' ±0.004	C_L ±0.016	A ±0.001
4	16.926	3.492	6.461	6.717	16.670	.962
10	16.925	3.491	6.460	6.717	16.668	.962
20	16.924	3.494	6.453	6.715	16.662	.961
30	16.920	3.500	6.440	6.710	16.650	.960
40	16.907	3.505	6.426	6.701	16.632	.959
50	16.889	3.515	6.409	6.687	16.611	.958
60	16.867	3.523	6.389	6.672	16.584	.958
70	16.840	3.532	6.367	6.654	16.553	.957
80	16.811	3.543	6.339	6.634	16.516	.956
90	16.776	3.554	6.309	6.611	16.474	.954
100	16.740	3.568	6.278	6.586	16.432	.953
110	16.698	3.582	6.248	6.558	16.388	.953
120	16.652	3.600	6.217	6.526	16.343	.953
130	16.597	3.613	6.187	6.492	16.292	.953
140	16.535	3.623	6.156	6.456	16.235	.954
150	16.460	3.624	6.126	6.418	16.168	.955
160	16.370	3.614	6.094	6.378	16.086	.955
170	16.301	3.635	6.075	6.333	16.043	.959
180	16.283	3.637	6.065	6.323	16.025	.959
190	16.264	3.640	6.055	6.312	16.007	.959
200	16.246	3.642	6.045	6.302	15.989	.959
210	16.227	3.645	6.035	6.291	15.971	.959
220	16.209	3.649	6.025	6.280	15.954	.959
230	16.189	3.653	6.015	6.268	15.936	.960
240	16.169	3.655	6.006	6.257	15.918	.960
250	16.149	3.659	5.996	6.245	15.900	.960
260	16.131	3.663	5.986	6.234	15.883	.960
270	16.109	3.667	5.977	6.221	15.865	.961
280	16.091	3.671	5.967	6.210	15.848	.961
290	16.072	3.676	5.957	6.198	15.831	.961
300	16.051	3.679	5.947	6.186	15.812	.961
0*	16.52 ±0.10	3.60 ±0.10	6.20 ±0.03	6.46 ±0.03	16.26 ±0.03	.96 ±0.02

*Extrapolated values for the disordered phase.

Possible variations in transit times due to changing domain alignments were investigated by measuring transit times for $GdAl_2$ at 77 K in magnetic fields of varying orientations. Within experimental precision the transit times were unaffected by the orientation of the magnetic field relative to the direction of wave propagation.

Errors resulting from thermal expansion are temperature dependent and corrections for these errors can be made if thermal expansion data are available. In the current investigation this error is zero at room temperature and probably increases monotonically with decreasing temperature to a maximum at 0 K. Thermal expansion data for the compounds under investigation are not available, so estimates were made of the probable maximum error in the elastic constants based on the behavior of other Laves phases. The thermal expansion data of Cheng (10) for $MgCu_2$ indicated a maximum correction of 0.5% for that compound while the data of Giegenack *et al.* (53) for $ZrCo_2$ resulted in a 0.2% maximum correction. These results for cubic Laves phases indicate a probable maximum correction on the order of 0.5%. *Ad hoc* corrections to the tabulated elastic constants can be made when thermal expansion data become available for these phases.

In addition to the thermal expansion error, additional errors in the elastic constants may arise from uncertainties in density, inaccuracies in sample geometry and orientation, variations in bond thickness, and uncertainties in transit time measurements. In the present investigation random errors arise dominantly as a result of uncertainties in transit time measurements. The precisions listed in Tables 3 through 6 are based

on this random error. The remaining considerations are largely systematic errors, and estimations of these errors indicated possible contributions of 0.29%, 0.25%, 0.21%, and 0.37% to the elastic constants of $CaAl_2$, YAl_2, $LaAl_2$, and $GdAl_2$, respectively.

As discussed by Huntington (33) the elastic constants of a metallic phase are normally expected to approach 0 K with zero slope and to show a monotonic decrease with increasing temperature. Zero slope at 0 K is required by the Third Law of Thermodynamics. The negative slope at higher temperatures is considered to result from two effects. The first is a lattice softening due to the increase in interatomic distances that is caused by thermal expansion. The second effect is the introduction of anharmonic interactions at higher temperatures resulting, in part, from the greater mean square displacement of atoms from their equilibrium positions. This normally expected thermal dependence can be modified by any of several additional contributions to lattice rigidity, e.g., magnetic or phase transformations. The elastic constants of MAl_2 compounds that are plotted in Figures 1 through 4 are seen to exhibit this normal temperature dependence except in the neighborhood of the magnetic transformation of $GdAl_2$. The temperature coefficient, T_{ij}, of the elastic constant, C_{ij}, is defined as

$$T_{ij} = \frac{1}{C_{ij}} \frac{dC_{ij}}{dT} , \qquad (11)$$

and values of the temperature coefficients at room temperature for $CaAl_2$, YAl_2, $LaAl_2$, and magnetically disordered $GdAl_2$ are listed in Table 7. Values of the temperature coefficients for magnetically ordered $GdAl_2$

Table 7. Room temperature values of $T_{ij} = (1/C_{ij})(dC_{ij}/dT)$ for MAl_2 phases in units of 10^{-4} deg^{-1}

Phase	T_{11}	T_{12}	T_{44}	T'	T_L
$CaAl_2$	-1.8	0	-2.5	-2.4	-1.7
YAl_2	-1.5	0	-1.8	-1.8	-1.4
$LaAl_2$	-1.2	0	-0.7	-1.6	-0.8
$GdAl_2$*	-1.2	+1.1	-1.7	-1.9	-1.2
$GdAl_2$**	-4.2	+2.8	-4.9	-5.6	-3.5

*Paramagnetic phase, T = 300 K.

**Ferromagnetic phase, T = 140 K.

were determined at 140 K and are included in Table 7. Coefficients for each normal mode are seen to be approximately equal for the phases at room temperature. The temperature coefficients for magnetically ordered $GdAl_2$ exhibit a threefold increase over those for the disordered phase.

As may be seen in Tables 3, 4, 5, and 6 the elastic anisotropy ratios for the MAl_2 compounds are all close to unity and essentially temperature independent. A low degree of anisotropy and temperature independent anisotropy are two strong indications that these phases are extremely stable. Although high anisotropy does not always indicate imminent instability (Li, Na, K, and Rb have anisotropy ratios (54, 55) in excess of 6.0), high values of anisotropy ratios that are highly temperature dependent (56, 57) or composition dependent (58) have been found to be harbingers of impending transformations. On the other hand phases with low, temperature independent anisotropy have shown little tendency towards phase transformations (56, 59).

DISCUSSION

Debye Temperature

The Debye temperature, θ, of a crystalline solid can be evaluated from the elastic constants. Methods for this evaluation have been reviewed by Alers (30). The major difficulty in the calculation arises from the necessity for averaging the elastic constants over a solid angle, and various methods differ in the rigor with which this average is determined. Overton and Schuch (60) have performed this averaging by a rigorous numerical integration of elastic constants over crystal space for cubic symmetry. Their results are presented in the form of extensive tables that can be used in the evaluation of Debye temperatures, θ_o, at 0 K. The rigor with which θ_o is calculated by this method is as good as the accuracy of the elastic constants. In comparison, the method of Anderson (61) evaluates the polycrystalline elastic moduli by the simple VRH procedure which is discussed in a subsequent section of this thesis. Values for θ_o are then derived with an isotropic approximation. The validity of θ_o calculated by Anderson's method depends upon the validity of the isotropic approximation as well as on accuracies of the elastic constants. For $CaAl_2$, YAl_2, $LaAl_2$, and $GdAl_2$ values for the Debye temperatures were calculated by the method of Overton and Schuch and by the method of Anderson. The maximum disagreement between the results of the two methods was 0.7^{o}. This agreement is not unexpected since the MAl_2 compounds have low shear anisotropy. Values for θ_o rounded to the nearest degree are shown in Table 8.

Debye temperatures for YAl_2, $LaAl_2$, and $LuAl_2$ are available from the

Table 8. Debye temperatures for AB_2 Laves phases and their constituent elements

AB_2	$\theta_o(A)$ (K)	$\theta_o(B)$ (K)	$\theta_o(AB_2)$ (K)	r_A/r_B
$CaAl_2$	234*	428**	474**	1.22
YAl_2	268*	428**	484**	1.19
$LaAl_2$ ***	142*	428**	374**	1.24
$GdAl_2$ md	170*	428**	399**	1.20
$GdAl_2$ mo	170*	428**	406**	1.20
$LuAl_2$	210*	428**	384*	1.17

*Debye temperature from specific heat data.

**Debye temperature from elastic constant data.

***md = magnetically disordered; mo = magnetically ordered.

specific heat data of Hungsberg and Gschneidner (16). Since θ_o from elasticity data is not available for $LuAl_2$, the value from specific heat data is included in Table 8. The θ_o from specific heat for YAl_2 and $LaAl_2$ are 473 and 352 K, respectively. These differ significantly from the θ_o from elasticity data and are not included in the table. Debye temperatures from specific heat data are normally evaluated from a linear fit of C_p/T *vs.* T^2. This approach is valid only at very low temperatures and assumes the absence of specific heat contributions other than lattice or electronic. The behavior of C_p for the RAl_2 phases is found to be considerably more complicated and normal evaluation of θ_o is precluded. Gschneidner (62) has re-examined these specific heat data and has found that numerical values of θ_o can be made to vary over a range of more than 50^o depending upon the number of terms in a polynomial fit of C_p/T *vs.* T^2. The best fit has been obtained with a more complex mathematical function which assumes a two-lattice model for RAl_2 compounds. The present interpretation of this behavior is that the lattice specific heat consists of contributions from two semi-independent sublattices, one for each atomic species. This point will be discussed further in conjunction with the bulk modulus.

Joseph and Gschneidner (29) have reported a correlation between the radius ratio, r_A/r_B, and the Debye temperature, θ_o, for an AB_2 Laves phase. The radius ratio that is calculated according to their method may be used to estimate the order of magnitude of the Debye temperature. If the radius ratio is less than the ideal value of 1.225, then, as noted on page 3, B-B contacts dominate the crystal and $\theta_o(AB_2)$ should be closer to

$\theta_o(B)$ than to $\theta_o(A)$. The converse is true for $r_A/r_B > 1.225$. A comparison of Debye temperatures is shown in Table 8. For this table, values for θ_o of Ca, Y, La, Gd, Lu, and Al were taken from the compilation of Gschneidner (63). Data in the table are consistent with the Joseph and Gschneidner correlation except for the case of $LaAl_2$. Atypical behavior by lanthanum compounds is not unusual and further examples of atypical behavior by $LaAl_2$ will be encountered in this thesis. The inference from Table 8 is that Al-Al bonds dominate the lattice vibrational behavior of the MAl_2 compounds.

Kittel (34) has shown that, if the crystal lattice is considered to consist of simple harmonic oscillators, the Debye temperatures for a series of isotypic compounds should vary inversely as the square root of the molecular weight, MW. Such proportionality is expected only if the interaction forces (spring constants) between atoms remain the same when an atom of one type is replaced by an atom of a different type. In this case, one can evaluate for each compound a characteristic constant, $k = \theta_o\sqrt{MW}$. Values of k for isotypic compounds with equivalent force interactions should be equal. Conversely if the interaction forces in a particular compound are different from those in the other compounds in the series, then the k for this compound will be atypical.

It is reasonable to expect the k values for YAl_2, $LaAl_2$, and $LuAl_2$ to be equal since Y, La, and Lu are all trivalent metals and should have essentially the same bonding electron configuration. It is also expected that $GdAl_2$ should have the same k value, if magnetic force contributions are excluded. The calculated values of k for YAl_2, magnetically disordered $GdAl_2$, and $LuAl_2$ are, in fact, nearly equal with $k = 5800 \pm 10$ deg

$(a.m.u.)^{\frac{1}{2}}$. The value for magnetically disordered $GdAl_2$ was determined from extrapolated values for the elastic constants. The k value for magnetically ordered $GdAl_2$ is 5910 $\pm$ 10 deg $(a.m.u.)^{\frac{1}{2}}$, from which one might infer that magnetic contributions are only about 2% of the total force constants. In contrast, the k value for $LaAl_2$ is 5200 $\pm$ 10 deg $(a.m.u.)^{\frac{1}{2}}$ which is nearly 12% lower than the mean k of the other three RAl_2 compounds. This is another example of atypical behavior by $LaAl_2$. Since calcium is divalent, one would expect the force constants in $CaAl_2$ to be weaker than those in RAl_2 compounds where R is trivalent. The value of k for $CaAl_2$, indeed, is found to be 4600 $\pm$ 10 deg $(a.m.u.)^{\frac{1}{2}}$ which is 25% lower than the value typical of RAl_2 compounds.

Electronic Considerations

Although it is generally conceded that size considerations are of dominant importance in determining the stability of Laves phases, it has been found that electronic considerations exert a modifying influence (64, 65, 66). These electronic considerations are Fermi surface-Brillouin zone (subsequently FSBZ) interactions. These interactions are sensitive to the degree of filling of the Brillouin zones and in this sense change with changing electron-to-atom, e/a, ratios. Psuedo-binary systems have been investigation in which successive regions of C15, C14, and C15 phase stability occur as the e/a ratios vary across the systems. Investigations of this type have been surveyed by Elliott and Rostoker (67) and by Dwight (68).

Studies involving RAl_2 phases were summarized in 1967 by Wallace and Craig (69) and more recent investigations of psuedo-binary RAl_2 systems

have been reported by Wallace and his co-workers (e.g., 20, 70, 71). These investigations indicate that cubic RAl_2 Laves phases are stable with e/a $\leq$ 1.3 or e/a $\geq$ 2.6. Between these regions of C15 stability lies a region of e/a ratios in which the hexagonal C14 phase is stable.

Values of the electron-to-atom ratio, the elastic anisotropy ratio, the polycrystalline Poisson's ratio, and K_e are presented in Table 9 for the MAl_2 compounds and for the other Laves phases for which elasticity data are available. The quantity, $K_e = C_{12} - C_{44}$, has been associated with the contribution of a free electron gas to the bulk modulus by de Launay (72). The groups into which the cubic compounds are divided were chosen because of the systematic differences that are seen in the parameters in Table 9.

Group I consists of compounds for which the electron-to-atom ratio, e/a, is greater than 2.6. These phases are all characterized by anisotropy ratios less than unity, by Poisson's ratios approximately equal to 0.2, and by negative values of K_e. These phases are the MAl_2 phases of the present investigation. Group II consists of compounds for which the electron-to-atom ratio, e/a, is less than or equal to 1.33. These phases are all characterized by anisotropy ratios greater than unity, by Poisson's ratios approximately equal to 0.3, and by positive values of K_e. Compounds in Group II, in contrast to those in Group I, all are seen to contain transition or noble metals with d-levels which probably contribute to the bonding energy but not to the conduction band.

It is readily apparent that Groups I and II are representative of the two regions of stability of cubic Laves phases. The FSBZ interactions

Table 9. Room temperature values of the anisotropy ratio, A, electron-to-atom ratio, e/a, polycrystalline Poisson's ratio, ν, and the free electron contribution to the bulk modulus, $C_{12} - C_{44}$, for various Laves phases

	e/a*	A	ν**	K_e***	Reference
Cubic Phases Group I					
$CaAl_2$	2.7	.98	.19	-1.42	-†
YAl_2	3.0	.82	.20	-2.22	-†
$LaAl_2$	3.0	.77	.22	-1.10	-†
$GdAl_2$	3.0	.96	.19	-2.27	-†
Cubic Phases Group II					
$ZrCo_2$	1.3	1.39	.29	+2.91	8
$HfCo_2$	1.3	1.36	.29	+3.30	8
UCo_2	$\leq$1.3††	1.41	.34	+6.12	9
$MgCu_2$	1.3	1.58	.33	+2.94	10
Hexagonal Phases					
$MgZn_2$	2.0	--	.28	--	12
$CaMg_2$	2.0	--	.23	--	11

*e/a was calculated by the use of the following valences: 1 for Cu; 2 for Ca, Mg, and Zn; 3 for Al, Y, La, and Gd; 4 for Zr and Hf; 0 for Co.

**ν is the VRH polycrystalline average for Poisson's ratio.

***$K_e = C_{12} - C_{44}$ in units of 10^{11} d/cm^2.

†This investigation.

††The e/a ratio for UCo_2 was calculated assuming a valence for U that is ≤ 4.

that have been shown (69) to be important in the considerations of phase stability involve different planes of the Brillouin zone for the two groups. This leads to different resistances to shear distortions, and, therefore, to systematically different values of the anisotropy ratios and Poisson's ratios for Groups I and II. K_e is also characteristically different for these groups, and must reflect a differing nature of deviation from the completely free electron gas approximation.

It may also be noted that Poisson's ratio is 0.28 for $MgZn_2$ which is comparable to values for the Group II cubic phases, while $CaMg_2$ has a value of 0.23 which is comparable to values for the Group I cubic phases. A rationale for this difference may again be d-levels. $CaMg_2$ has no such levels while the d-level contribution of Zn to $MgZn_2$ should lie in an energy range comparable to the d-level contribution of the noble and transition metals to their respective compounds.

The above electronic considerations have been observed in only a limited number of the known Laves phase compounds, e.g., MAl_2, MCo_2, etc. The observations are suggestive rather than conclusive. Further testing should be undertaken before generalizations can be made. Investigations should be made of phases not containing rare earths, aluminum, or cobalt, but the phases should be chosen to determine the relevance of the d-orbital correlations mentioned in the present study.

Polycrystalline Moduli

Although it is not, in general, possible to calculate the exact elastic behavior of a polycrystalline material from the single crystalline elastic constants, approximations of the polycrystalline moduli may be

obtained by averaging techniques. These have been reviewed by Huntington (33) and Anderson (61). Two early approximation procedures were developed by Voigt (73) and by Reuss (74). The first was developed with the assumption of homogeneous stress with averaging over strain. The second was developed with the assumption of homogeneous strain with averaging over stress. In a polycrystalline material it is not possible to maintain both homogeneous stress and homogeneous strain because of the constraints of grain boundaries. It is necessary, therefore, to compromise between the extremes, and Hill (75) has shown that the expected value of the polycrystalline modulus should fall between the Voigt and Reuss averages. Hill has proposed that the arithmetic average be taken as the best estimate of the polycrystalline elastic constants. This is referred to as a VRH average by Anderson (61). In Table 10 are presented the results of VRH averaging for $CaAl_2$, YAl_2, $LaAl_2$, and $GdAl_2$.

It has been postulated by Smith (76), and supporting data has been presented (8, 11, 12, 13, 56, 77), that the bulk modulus of an intermetallic compound A_xB_y can be estimated by the arithmetic average of the bulk moduli, K_A and K_B, of the constituent elements:

$$\bar{K} = \frac{xK_A + yK_B}{x + y} \quad . \tag{12}$$

Discrepancies between such estimated and experimental values are normally considered acceptable if less than 10%. In Table 11 is shown a comparison of estimated and experimental bulk moduli for a number of Laves phases. For the MAl_2 phases the data show that, except for $LaAl_2$, the discrepancies fall outside the acceptable limit. Indeed from the data in the table, it

Table 10. Polycrystalline moduli from VRH averaging of single crystalline elastic constants for MAl_2 phases. The bulk modulus, K, the shear modulus, μ, and Young's modulus, E, are in units of 10^{11} d/cm^2. Poisson's ratio, ν, is dimensionless

	T(K)	K	μ	E	ν
$CaAl_2$	4.2	4.85 ± 0.02	3.90 ± 0.01	9.23 ± 0.07	0.18 ± 0.01
	300	4.73 ± 0.02	3.69 ± 0.01	8.78 ± 0.07	0.19 ± 0.01
YAl_2	4.2	8.15 ± 0.02	6.32 ± 0.03	15.1 ± 0.1	0.19 ± 0.01
	300	7.96 ± 0.02	6.08 ± 0.03	14.5 ± 0.1	0.20 ± 0.01
$LaAl_2$	4.2	7.07 ± 0.01	4.90 ± 0.05	11.9 ± 0.1	0.22 ± 0.01
	300	6.92 ± 0.01	4.78 ± 0.05	11.7 ± 0.1	0.22 ± 0.01
$GdAl_2$	4.2	7.97 ± 0.03	6.56 ± 0.02	15.4 ± 0.1	0.18 ± 0.01
	300	7.80 ± 0.03	6.04 ± 0.02	14.4 ± 0.1	0.19 ± 0.01
$GdAl_2$*	0	7.91 ± 0.15	6.30 ± 0.15	14.9 ± 0.5	0.19 ± 0.02

*Extrapolated to 0 K for magnetically disordered phase.

is obvious that any averaging procedure for estimating bulk moduli for YAl_2 and $GdAl_2$ from elemental bulk moduli is precluded since the bulk moduli of the compounds are greater than either of the elemental moduli.

One interpretation of this behavior is that the bulk moduli of these phases are determined by the aluminum sublattice with added resistance to compressive deformation caused by an effective pressure provided by the rare earth sublattice. The effective pressure would only need to be a fraction of a kilobar since the values of the bulk moduli of YAl_2 and $GdAl_2$ are equivalent to the bulk modulus of aluminum under pressures of 0.22 and 0.3 kbar, respectively (78). Some support for this point of view is available from Debye temperature considerations. It has been previously shown that the Debye temperatures of the RAl_2 phases are such as to indicate that Al-Al bonds are predominant in the lattice. In addition the complex behavior found in specific heats has led to the conclusion that semi-independent sublattices may contribute to the specific heats of the RAl_2 compounds. The elastic and thermal data, then, are both in accord with a two-lattice model. In this model the aluminum sublattice supplies the dominant contribution to the bulk modulus and θ_o, and the rare earth sublattice has only a secondary role.

The two sublattice model seems to be less applicable for the other Laves phase compounds in the table since, with the sole exception of $MgCu_2$, the maximum discrepancy between the experimental and averaged bulk moduli is 5%. The large discrepancy for $MgCu_2$ is possibly related to the multiple valence states available for copper. Surprisingly, the value of the constant, $k = \theta_o\sqrt{MW}$, for $MgCu_2$ is 4.15 deg $(a.m.u.)^{\frac{1}{2}}$ and is almost

Table 11. Comparison of estimated and measured room temperature bulk moduli of Laves phases and their constituent elements in units of 10^{11} d/cm^2

AB_2	K_A†	K_B†	$\bar{K}$*	K_{AB_2}	% error	Reference
$CaAl_2$	1.71	7.78	5.79	4.73	+23	-***
YAl_2	4.15	7.78	6.60	7.96	-18	-***
$LaAl_2$	3.15	7.78	6.27	6.92	- 9	-***
$GdAl_2$	3.78	7.78	6.48	7.80	-17	-***
$ZrCo_2$	9.65	18.98	15.87	15.28	+ 4	8
$HfCo_2$	10.87	18.98	16.28	16.74	- 2	8
UCo_2	10.60	18.98	16.19	15.76	+ 5	9
$MgCu_2$	3.56	13.80	10.39	8.80	+17	10
$MgZn_2$**	3.56	7.24	6.04	5.94	+ 1	12
$CaMg_2$**	1.71	3.56	2.94	2.95	0	11

*$\bar{K} = (K_A + 2K_B)/3$.

**Hexagonal.

***This investigation.

†The elemental bulk moduli were calculated from single crystalline elastic constants from the compilations of Hearmon (1, 2) for Al, Co, Cu, Hf, Mg, Ti, U, Y, Zn, and Zr. The bulk moduli were calculated from the compressibilities reported by Smith (79) for Ca and by Smith, Carlson, and Spedding (80) for La and Gd.

exactly the same as the value of 4.11 deg $(a.m.u.)^{\frac{1}{2}}$ for $MgZn_2$. This is a possible indication of divalent copper in $MgCu_2$.

SUMMARY

The single crystalline elastic constants of the cubic Laves phase compounds $CaAl_2$, YAl_2, $LaAl_2$, and $GdAl_2$ have been determined over the temperature range 4.2 to 300 K by pulse-overlap techniques. The elastic constants generally exhibit a monotonic decrease with increasing temperature with no inflections. The only exception to this behavior is found in $GdAl_2$ as a result of a magnetic transformation at approximately 165 K. Over this region the slopes of the curves of elastic constant vs. temperature are found to increase by a factor of about three. Elastic anisotropy ratios were found to be nearly unity and essentially independent of temperature for these four phases.

The Debye temperatures were calculated from the elastic constants and were of such a magnitude as to indicate Al-Al contacts (in the rigid sphere approximation) for each of the MAl_2 compounds. In addition radius ratios generally indicated Al-Al contacts for the MAl_2 phases. Values of a constant, $k = \theta_o\sqrt{MW}$, which is indicative of the strength of interatomic interaction forces, were nearly equal for the RAl_2 compounds. This behavior indicates that the RAl_2 compounds have, in general, equivalent interaction forces. $LaAl_2$ was found to be atypical in both the radius ratio and interaction force correlations. The value of k for $CaAl_2$ was expected to be, and found to be, lower than those for RAl_2 compounds.

Polycrystalline elastic constants were calculated by VRH averaging of the single crystalline elastic constants. The bulk moduli of intermetallic compounds are often adequately estimated by the arithmetic average of the bulk moduli of their constituent elements. However, this estimate

of the bulk modulus is acceptable only for $LaAl_2$ among the MAl_2 compounds. Indeed, the bulk moduli of YAl_2 and $GdAl_2$ are larger than the elemental bulk moduli for Y, Gd, or Al. These data and the Debye temperature considerations both indicate that the aluminum sublattice provides the dominant contribution to the θ_o and bulk moduli of MAl_2 compounds. It is possible that a two-lattice model consisting of two semi-independent sublattices may best describe the behavior of these phases.

Investigation of electronic effects resulted in the separation of the cubic Laves phases into two distinct groups. These groups were characterized by distinctively different values of the electron-to-atom ratio, the anisotropy ratio, Poisson's ratio and the contribution of the free electron gas to the bulk modulus. The distinctive groupings result from changes in the Fermi surface-Brillouin zone interactions which reflect the different degrees of filling of the Brillouin zones. Alternatively, there may be an effect from the presence of a valence band originating from atomic d-levels. This latter possibility is based upon the observation that all phases in the second group have at least one component which is either a transition metal or a noble metal. On the basis of Poisson's ratio for the two hexagonal Laves phases for which elasticity data are available, it appears that further extension of this d-level correlation may be possible.

REFERENCES

1. R. F. S. Hearmon, in Landolt-Bornstein Tables, edited by K. H. Hellwege (Springer-Verlag, New York, 1966), New Series, Group III, Vol. 1, pp. 1-39.

2. R. F. S. Hearmon, in Landolt-Bornstein Tables, edited by K. H. Hellwege (Springer-Verlag, New York, 1969), New Series, Group III, Vol. 2, pp. 1-39.

3. W. B. Pearson, Handbook of Lattice Spacings and Structures of Metals and Alloys, Vol. 2, (Pergamon Press, New York, 1967), pp. 67-68.

4. J. B. Friauf, Phys. Rev. 29, 34-40 (1927).

5. J. B. Friauf, J. Amer. Chem. Soc. 49, 3107 (1927).

6. F. Laves and H. Witte, Metallwirt. 14, 645-649 (1935).

7. T. B. Massalski, in Theory of Alloy Phases, (ASM, Cleveland, Ohio, 1956), pp. 63-123.

8. G. W. Shannette and J. F. Smith, J. Appl. Phys. 40, 79-82 (1969).

9. E. D. Gibson, J. Appl. Phys. 38, 3026 (1967).

10. C. H. Cheng, J. Phys. Chem. Solids 28, 413-416 (1967).

11. A Sumer and J. F. Smith, J. Appl. Phys. 33, 2283-2286 (1962).

12. G. W. Shannette and J. F. Smith, Scripta Met. 3, 33-36 (1969).

13. G. W. Shannette and J. F. Smith, J. Appl. Phys. 42, 2799-2803 (1971).

14. C. Deenadas, A. W. Thompson, R. S. Craig, and W. E. Wallace, J. Phys. Chem. Solids 32, 1853-1866 (1971).

15. R. W. Hill and J. M. Machado da Silva, Phys. Lett. 30A, 13-14 (1969).

16. R. E. Hungsberg and K. A. Gschneidner, Jr., J. Phys. Chem. Solids 33, 401 (1972).

17. H. J. Van Daal and K. H. J. Buschow, Solid State Comm. 7, 217-221 (1969).

18. J. A. Mydosh, M. P. Kawatra, and J. I. Budnick, Phys. Lett. 24A, 421-422 (1967).

19. V. U. S. Rao and W. E. Wallace, Phys. Rev. B2, 4613-4616 (1970).

20. B. Leon, V. U. S. Rao, and W. E. Wallace, J. Less-Common Metals 24, 247-251 (1971).

21. V. Niculescu, I. Pop, and N. Rosenberg, Phys. Lett. 34A, 265-266 (1971).

22. H. Oesterreicher and W. E. Wallace, J. Less-Common Metals 13, 91-102 (1967).

23. R. G. Barnes, Phys. Rev. Lett. 6, 221-223 (1961).

24. V. Jaccarino, J. Appl. Phys. 32, 102s-106s (1961).

25. E. D. Jones and J. I. Budnick, J. Appl. Phys. 37, 1250-1251 (1966).

26. N. Nereson, C. Olsen, and G. Arnold, J. Appl. Phys. 37, 4575-4580 (1966).

27. N. Nereson, C. Olsen, and G. Arnold, J. Appl. Phys. 39, 4605-4609 (1968).

28. G. Will, Z. Naturforschung, 23a, 413-416 (1968).

29. R. R. Joseph and K. A. Gschneidner, Jr., Scripta Met. 2, 631-634 (1968).

30. G. W. Alers, Physical Acoustics 3B, 1-42 (1965).

31. A. E. H. Love, A Treatise on the Mathematical Theory of Elasticity (Dover Publications, New York, 1944).

32. J. F. Nye, Physical Properties of Crystals (Oxford University Press, London, 1969), pp. 82-142.

33. H. B. Huntington, Solid State Phys. 7, 213 (1958).

34. C. Kittel, Introduction to Solid State Physics, Third Edition, (John Wiley and Sons, Inc., New York, N.Y., 1966).

35. O. D. McMasters, Private Communication (1971).

36. W. B. Pearson, Handbook of Lattice Spacings and Structures of Metals and Alloys (Pergamon Press, New York, 1958), p. 317.

37. R. W. Meyerhoff, D. M. Bailey, and J. F. Smith, Rev. Sci. Instr. 32, 715-717 (1961).

38. Handbook of Chemistry and Physics, edited by C. D. Hodgman, (Chemical Rubber Publishing Co., Cleveland, Ohio, 1957), p. 353.

39. B. D. Cullity, Elements of X-ray Diffraction (Addison-Wesley, Reading, Mass., 1956), p. 464.

40. J. B. Nelson and D. P. Riley, Proc. Phys. Soc. (London) 57, 160 (1945).

41. H. Otte, J. Appl. Phys. 32, 1536 (1961).

42. N. C. Baenziger and J. L. Moriarty, Acta Cryst. 14, 948 (1961).

43. A. Iandelli, The Physical Chemistry of Metallic Solutions and Intermetallic Compounds (H. M. S. O., London, 1959), p. 3.

44. H. Nowotny and A. Mohrnheim, Z. Krist. 100, 540 (1939).

45. F. R. Eshelman, U. S. Atomic Energy Commission Report No. IS-2594 (1971).

46. J. E. May, Jr., IRE National Convention Rev. 6, Pt. 2, 134 (1958).

47. E. P. Papadakis, J. Acoust. Soc. Am. 42, 1045 (1967).

48. H. B. Huntington, Phys. Rev. 72, 321 (1947).

49. H. J. McSkimmin, J. Acoust. Soc. Am. 33, 12-16 (1961).

50. M. P. Kawatra and J. A. Mydosh, Phys. Lett. 28A, 182-183 (1968).

51. M. P. Kawatra, J. A. Mydosh, and J. I. Budnick, Phys. Rev. B2, 665-670 (1970).

52. H. J. Williams, J. H. Wernick, E. A. Nesbitt, and R. C. Sherwood, J. Phys. Soc. Japan 17, Supplement B-1, 91 (1962).

53. H. Giegenack, H. Schott, G. E. R. Schulze, and H. J. Ullrich, Phys. Status Solidi 14, K189-K193 (1966).

54. E. J. Gutman and J. Trivisonno, J. Phys. Chem. Solids 28, 805-809 (1967).

55. D. I. Bolef, J. Appl. Phys. 32, 100-105 (1961).

56. R. J. Schiltz, Jr., T. S. Prevender, and J. F. Smith, J. Appl. Phys. 42, 4680-4684 (1971).

57. S. Zirinsky, Acta Met. 4, 164-171 (1956).

58. D. B. Novotny and J. F. Smith, Acta Met. 13, 881-888 (1965).

59. D. I. Bolef, R. E. Smith, and J. G. Miller, Phys. Rev. B3, 4100-4108 (1971).

60. W. C. Overton, Jr., and A. F. Schuch, Los Alamos Rpt. LA-3615 (1966).

61. O. L. Anderson, J. Phys. Chem. Solids 24, 909-917 (1963).

62. K. A. Gschneidner, Jr., Private Communication (January, 1972).

63. K. A. Gschneidner, Jr., Solid State Physics 16, 275-426 (1964).

64. F. Laves and H. Witte, Metallwirt. 15, 15-22 (1935).

65. F. Laves and H. Witte, Metallwirt. 15, 840-842 (1936).

66. H. Klee and H. Witte, Z. Physikalische Chemie. 202, 352-378 (1954).

67. R. P. Elliott and W. Rostoker, Trans. ASM 50, 617-633 (1958).

68. A. E. Dwight, Trans. ASM 53, 479-500 (1961).

69. W. E. Wallace and R. S. Craig, in Phase Stability in Metals and Alloys, edited by P. S. Rudman, J. Stringer, and R. I. Jaffee (McGraw-Hill, New York, N.Y., 1967), pp. 255-272.

70. H. Oesterreicher and W. E. Wallace, J. Less-Common Metals 13, 91-102 (1967).

71. H. Oesterreicher, J. Appl. Phys. 42, 5137-5143 (1971).

72. J. de Launay, Solid State Physics 2, 219-303 (1956).

73. W. Voigt, Lehrbuch der Kristalphysik (Teubner, Leipzig, 1928), pp. 716-761.

74. A. Reuss, Z. Angew. Math. Mech. 9, 55 (1929).

75. R. Hill, Proc. Phys. Soc. (London) A65, 349 (1952).

76. J. F. Smith, in Nuclear Metallurgy, edited by J. T. Waber, P. Chiotti, and W. N. Miner (Edwards Bros., Ann Arbor, Mich., 1964), Vol. 10, p. 397.

77. M. L. Shepard and J. F. Smith, Acta Met. 15, 357-363 (1967).

78. D. Lazarus, Phys. Rev. 76, 545-553 (1949).

79. J. F. Smith, in Metals Handbook, Vol. 1, (American Society for Metals, Metals Park, Ohio, 1961), p. 1199.

80. J. F. Smith, C. E. Carlson, and F. H. Spedding, Trans. AIME 209, 1212-1213 (1957).

ACKNOWLEDGMENTS

I would like to dedicate this thesis to my wife, Jan, and to my children, Ron, Steve, Lorraine, and Lisa. Without their patience and understanding this thesis could not have been written.

I also wish to thank Dr. J. F. Smith for his direction and encouragement in this work and in several additional investigations during my term as a graduate student. I thank Dr. K. A. Gschneidner, Jr., for his encouragement, advice, and counsel. I am grateful to D. M. Bailey for his invaluable help in the X-ray and computational work and to O. D. McMasters for his help in the thermal analyses. It is also proper to acknowledge the assistance of F. N. Linder, A. Johnson, H. H. Baker, P. E. Palmer, G. Wells, and D. Woods, for without the benefits of their experience this research would have been a much more difficult task.